



Article submitted to journal

Subject Areas:

xxxx, xxxx, xxxx

Keywords:Standard Model, Higgs Boson,
Renormalization Group**Author for correspondence:**

Holger Gies

e-mail: holger.gies@uni-jena.deRenormalization Group Flow
of the Higgs PotentialHolger Gies^{1,2,3} and René Sondenheimer¹¹Theoretisch-Physikalisches Institut,
Friedrich-Schiller-Universität Jena, Max-Wien-Platz 1,
07743 Jena, Germany²Abbe Center of Photonics, Friedrich Schiller
University Jena, Max Wien Platz 1, 07743 Jena,
Germany³Helmholtz-Institut Jena, Fröbelstieg 3, D-07743 Jena,
Germany

We summarize results for local and global properties of the effective potential for the Higgs boson obtained from the functional renormalization group, which allows to describe the effective potential as a function of both scalar field amplitude and RG scale. This sheds light onto the limitations of standard estimates which rely on the identification of the two scales and helps clarifying the origin of a possible property of meta-stability of the Higgs potential. We demonstrate that the inclusion of higher-dimensional operators induced by an underlying theory at a high scale (GUT or Planck scale) can relax the conventional lower bound on the Higgs mass derived from the criterion of absolute stability.

1. Introduction

The measurement of the mass of the Higgs boson [1, 2] together with masses and couplings of the other standard model degrees of freedom has made it clear that the standard model happens to reside in a rather particular place in parameter space: extrapolating the renormalization running of the couplings to higher scales, all couplings (apart from the U(1) gauge coupling) tend to smaller values, possibly towards zero. The Higgs-field self coupling may even drop below zero, which is conventionally interpreted as a signature for a potential instability of the standard model occurring at a scale near $10^{10...12}$ GeV.

Since the standard model as a quantum field theory is conceptually defined in terms of a functional integral and a bare action that parametrizes the microscopic interactions, it is useful to look at the system from a top-down perspective starting from a high energy scale Λ , where the microscopic interactions are fixed. The long-range observables measured at colliders then are a result obtained after averaging over the fluctuations of all quantum degrees of freedom. Depending on the embedding into an underlying theory, Λ may be considered as a GUT-like scale or the Planck scale, or any other scale where degrees of freedom beyond the standard model contribute significantly to the dynamics. Technically, Λ may be viewed as a UV cutoff regularizing the highest energy scales where the standard model description does no longer apply anyway.

From this viewpoint, all long-range observables are fixed, once the bare action S_Λ is chosen. A convenient tool to bridge the gap between Λ and collider scales is the renormalization group (RG), quantifying the running of couplings and masses from the UV to the IR. Even in the weak coupling regime, the dependence of the IR observables on the bare parameters in S_Λ can be involved and requires the solution of the RG flow. Even before the first measurement of the Higgs mass, it has long been known that possible mass values are bounded by a finite interval, the IR window [3–9], once a set of parameters are fixed, most prominently the heaviest top quark mass.

The measured value of the Higgs mass appears to indicate that m_H is slightly below the lower bound imposed by demanding for absolute stability of the electroweak Fermi vacuum, while it is well inside the bound, if the Fermi minimum is permitted to be meta-stable but sufficiently long lived, see, e.g., [10,11]. While a precise location of the bound still requires a better accuracy for the determination of the top Yukawa coupling and the strong coupling constant [12], we wish to emphasize and quantify the influence of the bare action S_Λ that comes along with a large number of unknown and not directly measurable parameters. From the RG perspective, most of these parameters are RG irrelevant.

While the perturbative RG typically concentrates on the RG relevant operators, presupposing perturbative renormalizability, the functional RG can also account for power-counting irrelevant operators. As long as the UV scale Λ is finite, also the irrelevant operators can contribute to long-range observables and thus to the size of the IR window. By power-counting arguments, their influence on long-range observables is typically powerlaw suppressed. Nevertheless, we argue below that they do have a quantitative impact, e.g., on the precise location of the line separating the fully stable from the meta-stable case. In this sense, also the irrelevant operators can be essential when drawing conclusions about the fate of the universe as we know it.

2. Perturbative RG vs. fermion determinant

In order to keep the discussion simple, we use a toy model for the top-Higgs sector involving a Dirac fermion and a real scalar field, featuring a discrete chiral \mathbb{Z}_2 symmetry [13]. We parametrize the bare action as

$$S_\Lambda = \int d^4x \left[\frac{1}{2}(\partial_\mu \phi)^2 + U_\Lambda(\phi) + \bar{\psi}i\cancel{\partial}\psi + ih_\Lambda \phi \bar{\psi}\psi \right], \quad (2.1)$$

with a bare Yukawa coupling h_Λ and a bare potential U_Λ . This simple model shares many features relevant for the stability problem with the standard model. We comment on more extensive models and the standard model below.

A conventional simple estimate of the effective potential of the Higgs is given by using a Coleman-Weinberg inspired form of the potential,

$$U_{\text{eff}}(\phi) = -\frac{1}{2}\mu^2\phi^2 + \frac{1}{8}\lambda(\phi)\phi^4, \quad (2.2)$$

where the mass parameter μ is chosen such that the potential acquires a vacuum expectation value v at the Fermi scale $v \simeq 246\text{GeV}$. Here, $\lambda(\phi)$ is determined from RG-improved perturbation

theory, i.e., by integrating the β function of the coupling which reads to one-loop order

$$\partial_t \lambda = \frac{1}{16\pi^2} (9\lambda^2 + 8h^2\lambda - 16h^4), \quad \partial_t = k \frac{d}{dk}. \quad (2.3)$$

The integration of Eq. (2.3) results in the coupling being a function of the RG scale k . The effective coupling for the potential is then obtained by identifying the RG scale with the field amplitude $\lambda(k = \phi)$. While this procedure is quantitatively well justified in many cases (in particular in the absence of further relevant scales), it comes with a loss of information: as a matter of principle, the effective potential depends on both scales, the field amplitude ϕ and the RG scale k separately. In contrast to the estimate for the “single-scale” potential (2.2), we can keep track of both dependencies with the functional RG.

The insufficiency of the single-scale potential becomes obvious from the following puzzle: assuming that the top-Yukawa coupling h at some scale starts to dominate the flow towards the UV in Eq. (2.3), the flow of λ will decrease and can even drop below zero. Upon insertion into U_{eff} , this can result in an instability of the single-scale potential. This is the standard argument for the occurrence of an instability also in the standard model.

Alternatively, we may not remain on the simple level of Eq. (2.3), but compute the full top-quark contribution to the effective potential to one-loop order. This is given by the fermion determinant,

$$U_F = -\frac{1}{2\Omega} \ln \frac{\det_{\Lambda}(-\partial^2 + h^2\phi^2)}{\det_{\Lambda}(-\partial^2)}, \quad (2.4)$$

where Ω denotes the spacetime volume, and the subscript Λ should remind us of the fact that a regularization at the cutoff scale is necessary. The determinant can be worked out exactly. For instance, for simple momentum-cutoff regularization, we get [14]

$$U_F = -\frac{\Lambda^2}{8\pi^2} h^2 \phi^2 + \frac{1}{16\pi^2} \left[h^4 \phi^4 \ln \left(1 + \frac{\Lambda^2}{h^2 \phi^2} \right) + h^2 \phi^2 \Lambda^2 - \Lambda^4 \ln \left(1 + \frac{h^2 \phi^2}{\Lambda^2} \right) \right]. \quad (2.5)$$

We observe a negative mass term $\sim \phi^2$. This is expected and ultimately absorbed in the renormalization of the mass-like parameter that fixes the Fermi scale as the vacuum expectation value v of the potential. Most importantly, the complete remainder being the interaction part of the potential is manifestly positive at any finite field amplitude.

The obvious puzzle now is that the same cause, namely the fermionic fluctuations, seems to lead to two different effects: the reasoning based on the single-scale potential suggests an instability for large Yukawa coupling, whereas the fermions contribute strictly positively to the full interaction potential in Eq. (2.5).

The puzzle is resolved by noting that the exact result for U_F also keeps track of the cutoff Λ dependence which remains invisible in the single-scale approach [13–17]. While perturbative renormalizability seems to suggest that the cutoff can be removed by renormalization conditions, it cannot be sent to infinity in the standard model because of its triviality problem in the U(1) sector. Hence, Λ is a (place holder for a) physical scale which should be kept track of.

It is instructive to try to reconcile the two contrary ends of the puzzle. For this, we may naively expand the interaction part of the potential (2.5) in powers of $h^2 \phi^2 / \Lambda^2$ for large Λ . Then we may absorb the $\log \Lambda$ divergence into a renormalization of λ , introducing a renormalization scale $\Lambda \rightarrow k$, and end up with

$$U_F|_{\phi^4} \stackrel{?}{=} -\frac{1}{16\pi^2} h^4 \phi^4 \ln \frac{h^2 \phi^2}{k^2} + \mathcal{O} \left(\frac{h^2 \phi^2}{\Lambda^2} \right). \quad (2.6)$$

This in fact looks like an unstable interaction potential for large ϕ (in obvious contradiction with (2.5)). This corollary of the original puzzle is resolved by noting that the instability sets in for large fields where $\left(\frac{h^2 \phi^2}{\Lambda^2} \right) \sim \mathcal{O}(1)$, i.e., where the large- Λ expansion is no longer justified. We emphasize that our line of argument does not rely on the momentum-cutoff regularization, but is identical for gauge-invariant regulators such as proper-time or zeta function regularization. Some care is required for dimensional regularization which fails to keep track of the explicit cutoff

dependence, since it is a projection (on log divergencies) rather than a regularization scheme. For details, see [14].

To summarize: In order to get global information about the stability of the Higgs effective potential in the standard model, it is advisable to (i) keep track of the cutoff Λ or the RG scale explicitly, and (ii) study the features of the potential globally. Both aspects can be taken care of with the functional RG.

3. Higgs mass bounds as a UV to IR mapping

Since we keep the cutoff finite in our analysis, we can also use it as our explicit renormalization scale where we fix all parameters of the theory in the form of specifying the microscopic action S_Λ . As there is no direct experimental information available about the parameters in this action, we may start from a generic action

$$\begin{aligned} S_\Lambda &= S_\Lambda(m_\Lambda^2, \lambda_{2,\Lambda}, \lambda_{3,\Lambda}, \dots, h_\Lambda, \dots) \\ &= \dots + \frac{1}{2}m_\Lambda^2\phi^2 + \frac{1}{8}\lambda_{2,\Lambda}\phi^4 + \frac{1}{48}\frac{\lambda_{3,\Lambda}}{\Lambda^2}\phi^6 + \dots + ih_\Lambda\phi\bar{\psi}\psi + \dots \end{aligned} \quad (3.1)$$

that includes higher-order operators such as $\sim \lambda_{3,\Lambda}\phi^6$, etc. On the level of the bare action, they are not forbidden at all. In fact, phenomenological studies involving such operators are common in this context [18–23]. Wilson’s powercounting arguments of renormalization tell us that these higher-order operators die out rapidly toward the IR and thus do not exert a sizable influence on the long-range observables (as long as the flow is dominated by the weak-coupling Gaussian fixed point regime). Still, these operators can exert an influence on the IR flow itself. The renormalization flow, i.e., averaging over the fluctuations of all quantum fields, now provides a mapping of the bare action onto the renormalized effective action $S_\Lambda \rightarrow \Gamma$. The latter encodes the dynamics of the theory in the IR and thus can be more directly parametrized in terms of the long-range observables. Any measured quantity therefore imposes a constraint on the form of Γ and thus indirectly on the form of S_Λ .

In the present work, we use the expectation value of the Higgs field $v \simeq 246\text{GeV}$ and the top quark mass $m_t \simeq 173\text{GeV}$ as input. This fixes two parameters of the bare action S_Λ , e.g. m_Λ^2 and h_Λ , but leaves the mass of the Higgs boson as a function of all other parameters of the bare action and of the cutoff itself, $m_H = m_H[S_\Lambda; \Lambda]$. The underlying mapping $S_\Lambda \rightarrow \Gamma$ can be approximated in various ways, e.g. perturbatively in the weak-coupling regime. Most useful in this regime are also a mean-field or extended-mean-field approximation which lead to fully analytical results, see [13]. A more comprehensive picture is obtained with the functional RG, yielding trustworthy results also at stronger coupling.

The functional RG can be formulated in terms of a flow equation for the effective action Γ_k interpolating between the bare action $\Gamma_{k=\Lambda} = S_\Lambda$ and the 1PI effective action $\Gamma = \Gamma_{k=0}$. This flow is obtained as the solution to the Wetterich equation [24],

$$\partial_t \Gamma_k = \frac{1}{2} \text{Tr} \left[(\Gamma_k^{(2)} + R_k)^{-1} \partial_t R_k \right], \quad \partial_t = k \frac{d}{dk}, \quad (3.2)$$

where R_k is a regulator specifying the details of the Wilsonian regularization near the momentum shell $p \simeq k$, and $\Gamma_k^{(2)} + R_k$ is the full inverse propagator at scale k , for details see [25–29]. We solve the flow in the space of actions that can be parametrized by

$$\Gamma_k = \int d^4x \left(\frac{Z_{\phi,k}}{2} (\partial_\mu \phi)^2 + U_k(\phi) + Z_{\psi,k} \bar{\psi} i \not{\partial} \psi + ih_k \phi \bar{\psi} \psi \right), \quad (3.3)$$

where the wave function renormalizations $Z_{\phi/\psi,k}$, the full potential U_k , and the Yukawa coupling h_k flow with the RG. Solving the flow with S_Λ as UV boundary condition (and fixing the expectation value v and the top mass m_t), we can read off the Higgs mass as the curvature of the (renormalized) potential at the minimum $m_H^2 = U''_{k \rightarrow 0}(v)/Z_{\phi,k \rightarrow 0}$.

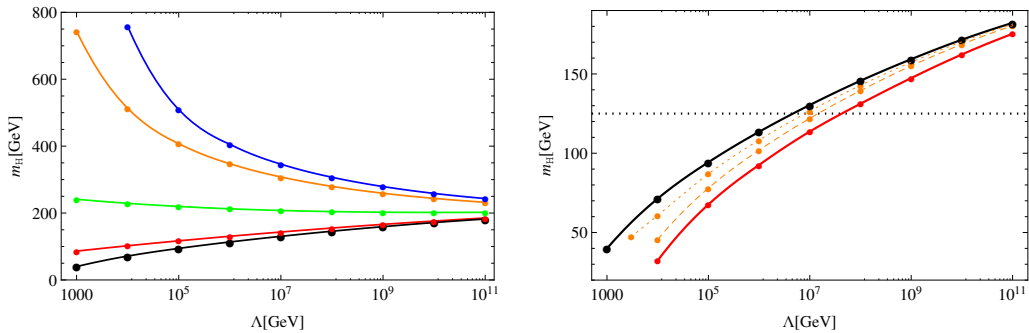


Figure 1. Left: Higgs mass $m_H(\lambda_{2,A}; \Lambda)$ versus cutoff Λ for a ϕ^4 -type bare potential for $\lambda_{2,A} = 0$ (black, lower bound) and $\lambda_{2,A} = 0.1, 1, 10, 100$ from bottom to top (red to blue). Right: “lower bound” with a ϕ^4 -type bare potential (black) in comparison with Higgs masses obtained with an inclusion of a bare $\lambda_{3,A}\phi^6$ operator (red line); intermediate orange dashed lines correspond to $\lambda_{3,A} = 3$ and $\lambda_{2,A} = -0.05, -0.08$. The “lower bound” can clearly be relaxed; the data agrees with [13].

Restricting the bare actions to the “renormalizable operators” of Eq. (2.1), i.e., $U_\Lambda = \frac{1}{2}m_\Lambda^2\phi^2 + \frac{1}{8}\lambda_{2,\Lambda}\phi^4$, the only remaining parameter after fixing v and m_t is the ϕ^4 coupling, such that $m_H = m_H(\lambda_{2,\Lambda}; \Lambda)$. The resulting Higgs masses in this model are shown in Fig. 1 (left panel) as a function of the cutoff Λ for various couplings $\lambda_{2,\Lambda}$ ranging from zero to the strong coupling region. Though m_H increases monotonically with $\lambda_{2,\Lambda}$, we observe that a finite IR window of possible Higgs masses emerges as a result of the flow. In the present toy model, the center of this window lies in the region $\simeq 200 \dots 250$ GeV. The lower bound is given by $\lambda_{2,\Lambda} = 0$. Our data indicates that the resulting Higgs mass also asymptotically approaches an upper Higgs mass bound for increasing couplings $\lambda_{2,\Lambda}$ for larger cutoffs Λ . In this class of bare ϕ^4 potentials, the lower bound $\lambda_{2,\Lambda} = 0$ is dictated by the existence of a well defined functional integral and thus corresponds to the criterion of absolute stability in this class.

However, the restriction to ϕ^4 potentials is arbitrary; neither formal renormalizability arguments nor experimental data serve to justify such a limitation. As a simple generalization, let us consider the next higher-order operator in the potential $\sim \lambda_{3,\Lambda}\phi^6$. In fact, many further operators can be (and have been) studied, see, e.g., [30,31] for higher-order fermionic operators or [32] for mixed operators. The present simple ϕ^6 example suffices to illustrate an important point here. The stability criterion $\lambda_{2,\Lambda} \geq 0$ of the ϕ^4 potentials can, of course, be alleviated by an inclusion of a coupling $\lambda_{3,\Lambda} > 0$. In particular, we can start with a negative $\lambda_{2,\Lambda}$ in the UV which turns into a positive $\lambda_{2,k}$ at lower scales by the RG flow, while $\lambda_{3,k}$ becomes small according to power counting. We observe that we obtain potentials which are fully stable on all scales but lead to lower Higgs masses than the “lower bound” obtained with ϕ^4 potentials, see Fig. 1 (right panel). This demonstrates that the conventional lower bound with ϕ^4 bare potentials can be relaxed upon the inclusion of higher-dimensional operators at the cutoff without losing absolute stability.

Our example suggests that the conventional lower bound should be replaced by a *consistency* bound defined by the smallest possible value for the Higgs mass as a function of the cutoff Λ , derived from the set of all possible microscopic bare actions S_Λ which define a consistent functional integral and are compatible with an absolutely stable Fermi minimum. Of course, computing the bound is a complicated minimization problem in an infinite dimensional space of bare actions with nontrivial constraints. The lower Higgs masses (red line) in Fig. 1 (right panel) thus represent merely a simple example that this consistency bound is below the conventional lower bound.

We also observe in this figure that our red-line example appears to approach the conventional lower bound (black line) for increasing cutoff values Λ . This is natural for flows in the vicinity of

the weak-coupling Gaussian fixed point: here, the higher-order operators are power-law depleted by the RG flow. Typically at scales of $k \sim 10^{-1 \dots 3} \Lambda$, the higher-dimensional operators do no longer contribute significantly to the flow which thus runs essentially close to that of the ϕ^4 -class towards the IR. Hence, the possible shift of the bound in the Higgs mass Δm_H also is a decreasing function of Λ under the assumption of weak coupling.

4. Towards the standard model

We have verified that the mechanism described above that leads to consistency bounds below the conventional stability bounds of the Higgs boson mass is also active in other models sharing further similarities with the standard model. The typical chiral structure of the standard model can, for instance, be tested with a correspondingly chiral model with a Yukawa sector coupling a complex SU(2) scalar doublet ϕ to a left-handed fermion top-bottom doublet $\psi_L = (t_L, b_L)$ and the corresponding right handed singlets t_R, b_R ,

$$S_{\Lambda, \text{Yuk}} = \int d^4x \left[i h_{b, \Lambda} (\bar{\psi}_L \phi b_R + \bar{b}_R \phi^\dagger \psi_L) + i h_{t, \Lambda} (\bar{\psi}_L \phi_C t_R + \bar{t}_R \phi_C^\dagger \psi_L) \right], \quad (4.1)$$

featuring the chiral SU(2) symmetry and giving room for two different Yukawa couplings h_t and h_b ; here $\phi_C = i\sigma_2 \phi^*$ is the charge conjugated scalar. The measured mass of the bottom quark $m_b \simeq 4.2 \text{ GeV}$ is used to implicitly fix the UV initial condition for the bottom Yukawa coupling at the cutoff scale $h_{b, \Lambda}$.

It is instructive, to first study the IR window, i.e., the range of accessible values for the Higgs mass within the class of bare ϕ^4 potentials [14]. The result is shown in Fig. 2 (left panel) (black solid lines for $\lambda_{2, \Lambda} = 0$ and $\lambda_{2, \Lambda} = 100$) and compared to the \mathbb{Z}_2 -symmetric model (red dashed lines) studied before. We observe that the conventional lower bound of the two models are almost identical. This confirms the usefulness of the simple \mathbb{Z}_2 Yukawa model for the purpose of studying the lower bound. The reason for this agreement simply lies in the fact that the bottom Yukawa coupling is much smaller than that of the top quark, with the latter dominating the dynamics near the lower bound. The situation is different at large Higgs self-coupling: here, the different number of scalar degrees of freedom plays a substantial role which leads to a narrowing of the IR window, now having its center near 200 GeV.

This model is also of interest, because it is used for nonperturbative studies of the Higgs mass bounds in lattice simulations [34–37]. The chiral gauge structure of the standard model is so far not accessible on the lattice, but this chiral model suffices to address quantitative questions, while extrapolating to the full standard model with the aid of perturbation theory. In fact, the same mechanism for relaxing the conventional lower bound by means of higher-order operators that we discovered for the \mathbb{Z}_2 model is also active in this chiral model [13, 14]; the corresponding plot upon an inclusion of a $\sim \lambda_{3, \Lambda} (\phi^\dagger \phi)^3$ operator looks identical to Fig. 1 (right panel), see Fig. 4 in [14]. The existence of this mechanism is also confirmed by lattice studies [38–41], corroborating the functional RG studies.

The chiral model nevertheless has a technical disadvantage, as the chirally broken (Fermi) phase necessarily goes along with the appearance of massless Goldstone modes. In the full standard model, they disappear through the Higgs mechanism, while they have to be removed by hand in the model studies both on the lattice as well as in the functional RG studies. This introduces a quantitatively small degree of model dependence which cannot be removed as a matter of principle. In order to avoid the full complexity of the standard model, but nevertheless acquire quantitatively relevant results, a hybrid model has been constructed in [33] that features a simple scalar \mathbb{Z}_2 sector, but includes the QCD gauge group SU(3) under which the fermions are charged,

$$S_\Lambda = \int_x \left[\frac{1}{4} F_{\mu\nu}^a F_{a\mu\nu} + \frac{1}{2} (\partial_\mu \phi)^2 + U_\Lambda(\phi) + \bar{\psi} i \not{D}[A] \psi + i h_\Lambda \phi \bar{\psi}_t \psi_t \right], \quad (4.2)$$

but only the top quark has a non-negligible Yukawa coupling to the Higgs scalar. In addition, the influence of the SU(2) and U(1) gauge group can be modeled on the level of the perturbative

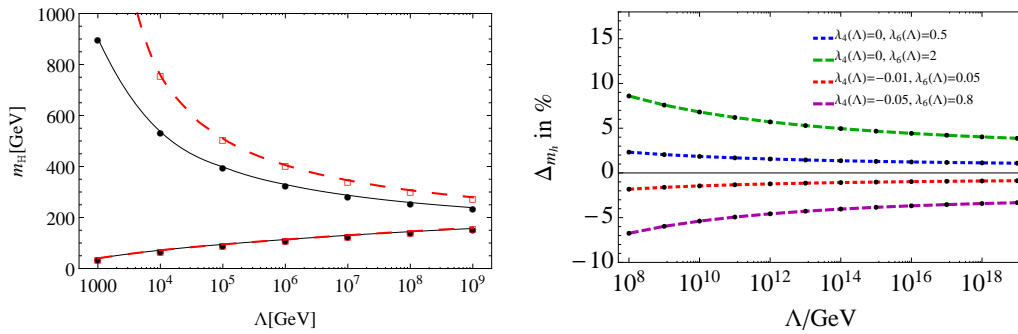


Figure 2. Left: Higgs mass $m_H(\lambda_{2,A}; \Lambda)$ versus cutoff Λ for a ϕ^4 -type bare potential for $\lambda_{2,A} = 0$ and $\lambda_{2,A} = 100$ (bottom to top) for the chiral Yukawa model (solid black line) in comparison with the \mathbb{Z}_2 model (red dashed line); taken from [14]. Right: relative mass shift of the Higgs boson mass compared to the conventional lower bound versus cutoff Λ upon the inclusion of higher-dimensional operators. The plot is based on a hybrid model introduced in [33] which quantitatively mimics the standard model flow in the Higgs sector. The solid black zero line hence corresponds to $m_H \simeq 129$ GeV at the Planck scale, and to $m_H \simeq 125$ GeV near $\Lambda \simeq 10^{10}$ GeV. The lowest curve accommodates the difference between the conventional lower bound and the measured Higgs mass even with Planck-scale operators, but corresponds to a metastable Fermi minimum. Higgs masses below the conventional lower bounds ($\Delta m_H < 0$) and a fully stable Fermi minimum can be found by our mechanism with suitable higher-dimensional scale terms in the bare action (red short-dashed line); taken from [33] with conventions $\lambda_6(\Lambda) = \lambda_{3,A}/6$.

beta functions. We have shown that the running of perturbatively renormalizable couplings in the relevant top-Higgs sector of this hybrid model can indeed be mapped onto that of the full standard model [33].

In this gauged model, the mechanisms induced by higher-order operators affecting the conventional lower Higgs-mass bound work much in the same way as in the Yukawa models discussed above. Still, one quantitative difference arises from the fact that the flow of the top Yukawa coupling receives an important contribution from the gauge sector, such that it behaves like an asymptotically free coupling in the region between the Fermi and, say, the Planck scale. Therefore, also the strong influence of the top quark fluctuations on the running of the scalar potential is somewhat reduced. In total, this leads to a flattening out of the lower Higgs mass curves a la Fig. 1 (right panel) toward larger cutoffs as well as to an IR window centered near smaller Higgs masses. For the standard model (as well as for our hybrid model), the center of the IR window is near $\simeq 130 \dots 150$ GeV. The conventional lower bound of the Higgs mass has been under intense investigation in recent years. The precise value, say for Λ equals the Planck mass, depends on the value of the Yukawa coupling (and to some degree on the value of the strong coupling constant and heavy gauge boson masses) [10,11,42]. Translating the measured value of the top mass straightforwardly into the Yukawa coupling leads to a conventional lower bound for absolute stability of $\simeq 129$ GeV [10,43] which demonstrates the tension with the measured value near 125 GeV. One important open question is that of the true quantitative relation between the top mass extracted from collider data and the corresponding top Yukawa coupling which appears to be inflicted by intrinsic uncertainties [12,44].

In order to study whether the lower-lying consistency bound permits for stability of the Higgs potential even for the measured low mass of the Higgs boson, we have determined the influence of the higher-order operators $\sim \lambda_{3,A} \phi^6, \dots$ of the scalar potential onto the lower bound [33]. As a quantitative measure, we have extracted the shift of the Higgs boson mass relative to the conventional lower bound as a function of $\lambda_{2,A}$ and $\lambda_{3,A}$. This shift is displayed in Fig. 2 (right panel) for various initial conditions over a wide range of cutoffs up to the Planck scale. The red short-dashed line shows an example with a negative value for $\lambda_{2,A}$, but a stabilizing positive $\lambda_{3,A}$

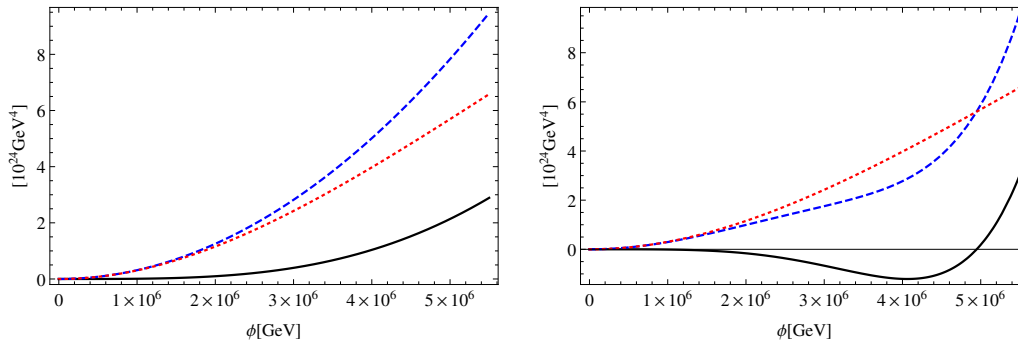


Figure 3. Effective mean-field potential (solid line) arising from the bare potential (blue long-dashed line) and the top-quark fluctuations (minus the fermion determinant) (red short-dashed). The effective potential has a minimum at the Fermi scale, $v = 246\text{GeV}$ (hardly visible on this scale). Left: initial conditions in the class of ϕ^4 -potentials, $\lambda_{2,A} = 0$, $\lambda_{3,A} = 0$. Right: metastability seeded by the bare action with $\lambda_{2,A} = -0.15$, $\lambda_{3,A} = 3$, $\Lambda = 10^7\text{GeV}$; taken from [45].

arranged such that the effective potential stays stable over all scales. With this example using the model of Eq. (4.2) or its hybrid version of [33] that exhibits all relevant standard model features, we can reach Higgs masses $\sim 1\%$, i.e., $\simeq 1\text{GeV}$ below the conventional lower bound for a cutoff at the Planck scale. Staying during the full flow within both the Gaussian weak coupling fixed point regime as well as within the class of a stable Fermi minimum, this $\mathcal{O}(1\%)$ mass shift appears to be a generic relaxation of the conventional lower bound inducible by Planck scale operators.

Whether initial conditions away from the Gaussian weak coupling fixed point can lead to a controlled flow with much lower Higgs masses is an open and equally interesting question. A mass shift of the order of 5% is straightforwardly possible, if a potential with a metastable (but possibly long-lived) Fermi minimum is acceptable. An example is given by parameters leading to the long-dashed purple line in Fig. 2 (right panel), cf. the discussion in the next section. The further two examples in Fig. 2 (right panel) show that non-vanishing Planck scale higher-order operators with $\lambda_{2,A} = 0$ but $\lambda_{3,A} > 0$ can also induce a positive mass shift and thus would possibly increase the tension between the observed value of the Higgs boson mass and Planck scale UV completions leading to such a bare action.

5. Higgs potentials with metastable Fermi vacuum

Our results so far proof that the details of the microscopic bare action, e.g., Planck scale operators, can take a significant and quantifiable influence on the lower mass bound for the Higgs boson – even if we insist on absolute stability of the Fermi vacuum. Within the conventional perturbative picture, the standard model appears to be below the conventional lower bound in a meta-stable but sufficiently long-lived region. This means that the single-scale potential exhibits another global minimum at large fields in addition to the Fermi minimum.

Though our results clearly shift the boundary between the stable and the metastable parameter region, they, of course, do not exclude the possibility of a metastable potential. Still, there seems to be a puzzle: in Eq. (2.5), we have shown that the interaction part of the fermion determinant contributes strictly positively to the scalar potential. Since the top-fluctuations dominate near the lower bound, how can a second deeper minimum be generated?

In fact, for microscopic actions with ϕ^4 bare potentials, this is not possible provided we start from a well-defined functional integral requiring $\lambda_{2,A} \geq 0$. This is illustrated at the mean-field level in Fig. 3 (left panel) for our simple Yukawa model, where the blue long-dashed line denotes the bare potential with a mass parameter fixed such that the effective potential (solid black line) has a proper single Fermi minimum at $v \simeq 246\text{GeV}$ (not well visible on this scale), and $\lambda_{2,A}, \lambda_{3,A}, \dots = 0$. The red short-dashed line denotes (minus) the fermion determinant which at

mean-field level needs to be subtracted from the bare potential to yield the effective potential. The resulting effective potential is globally stable with one minimum at the Fermi scale [45].

By contrast, the right panel of Fig. 3 starts from a bare action with parameters adjusted such that the bare potential exhibits a kink (at $\phi \sim 4 \times 10^6 \text{ GeV}$ in this example). This bare potential still has only one minimum at $\phi = 0$, but in combination with the contributions from the top-fluctuations (fermion determinant), the effective potential exhibits two minima, one near the kink position seeded in the bare action and the second one being the Fermi minimum by construction (again not well visible on this scale). We conclude that metastabilities can, of course, occur in the Higgs sector also in the class of consistent bare actions [45]. The important point is that this metastability of the Fermi minimum by a second deeper minimum at large fields has to be seeded by corresponding structures in the bare action. The latter would have to be provided by the underlying theory.

While the mean-field approximation is capable of illustrating these stability/meta-stability features rather well, it does not establish convexity as is obvious from Fig. 3 (right). In fact, from the definition of the effective action as a Legendre transform, convexity is a built-in property of the effective potential, which is respected neither at mean-field level nor in conventional perturbation theory. It is thus a natural question as to whether the convexity property of the potential has any decisive influence on the picture developed so far?

As a powerful feature, the structure of the Wetterich equation (3.2) does establish convexity of the potential for its global solutions [46]. We have analyzed this approach to convexity quantitatively in the present model in [45]. Our results demonstrate that the convexity generating mechanisms set in in the deep infrared below the scale where the top quark decouples and the Fermi minimum forms. For all cases studied in [45], there is a clear separation between the regime where the electroweak mass spectrum arises and the IR regime where convexity sets in. Hence, we expect convexity to be essentially irrelevant for the mass spectrum, whereas its influence on vacuum-decay-rate calculations deserves a more detailed study.

6. Conclusion

We have reconsidered the conventional reasoning for the computation of bounds on the Higgs mass arising from the assumption that the standard model provides a quantitatively valid description of nature up to some high-energy scale Λ . Because of our ignorance of the physics at that scale Λ , the microscopic action S_Λ serving as a UV boundary condition is largely undetermined. As a consequence, higher-dimensional operators have to be expected to be present at the high scale. While these operators do not take a direct influence on long-range observables provided the standard model is close to the weak-coupling fixed point, they can modify the RG flow near the high scale, leaving an indirect imprint on low-energy physics.

We have illustrated these findings with the example of consistent (effective) field theories that allow for Higgs boson masses below the conventional lower bound. This mechanism triggered by higher-dimensional operators is also present in the standard model. Our estimates based on a variety of model studies suggest that even Planck scale operators can induce a relaxation of the conventional lower bound on the order of 1% for the absolute stability bound. While we have considered here the influence of only one ϕ^6 -type operator as an example, similar features occur, for instance, upon the inclusion of higher-order fermionic operators [30,31] or mixed operators [32] as well as in theories with additional scalar fields, e.g., dark matter candidates [47]. Most of the quantitative studies so far have explored only initial conditions which are already sufficiently close to the Gaussian fixed point. We emphasize that it remains an interesting open question to study how far the true consistency bounds can be pushed if also strongly coupled regions are included in the analysis. The functional RG advocated in this work is ideally suited for this problem.

Since even the conventional estimates are compatible with a metastable but sufficiently long-lived Higgs vacuum state, it is a legitimate question as to whether there is any relevant difference for contemporary phenomenology, depending on which scenario is ultimately realized. In fact,

the interplay between stability, metastability and cosmology is currently actively studied within various cosmological models [42,48–52]. If such considerations favored absolute stability but the tension with the observed Higgs mass and the conventional bounds persisted, this could point to new physics below the Planck scale (according to the conventional interpretation) or correspond to a first measurement of properties of the microscopic action with a sufficiently deep consistency bound. With respect to cosmology, also the thermal evolution of the Higgs potential is of substantial interest. In this respect, higher-dimensional operators can also exert an influence on the nature of the thermal phase transition, as has already been observed in lattice simulations [53]. It is an interesting question as to whether the set of bare actions contains relevant microscopic initial conditions for which the electroweak phase transition is sufficiently strongly first order in order to support electroweak baryogenesis.

A particularly fascinating scenario would arise, if the Higgs boson mass happened to lie close to the value that corresponds to an exactly flat interaction potential. Then the UV theory has to guarantee such an exceptional matching condition at the high scale. In fact, asymptotically safe gravity had been suggested for such a scenario already before the discovery of the Higgs boson [54], see also [55]. Purely within particle field theory, such a scenario would be most natural in theories where also the Higgs sector becomes asymptotically free – a long-standing idea that currently witnesses new attraction [56–60].

Funding. This work received funding support by the DFG under Grants No. GRK1523/2 and No. Gi328/7-1. R.S. acknowledges support by the Carl-Zeiss foundation.

Acknowledgements. We are grateful to J. Borchardt, A. Eichhorn, C. Gneiting, J. Jaeckel, T. Plehn, M.M. Scherer, and M. Warschinke for collaboration on various parts of the topic. We thank A. Rajantje, M. Fairbairn, T. Markkanen, and A. Eichhorn for their efforts in organizing this productive and enjoyable workshop.

References

1. Aad G, et al.
Observation of a new particle in the search for the Standard Model Higgs boson with the ATLAS detector at the LHC.
Phys Lett. 2012;B716:1–29.
2. Chatrchyan S, et al.
Observation of a new boson at a mass of 125 GeV with the CMS experiment at the LHC.
Phys Lett. 2012;B716:30–61.
3. Maiani L, Parisi G, Petronzio R.
Bounds on the Number and Masses of Quarks and Leptons.
Nucl Phys. 1978;B136:115.
4. Krasnikov NV.
Restriction of the Fermion Mass in Gauge Theories of Weak and Electromagnetic Interactions.
Yad Fiz. 1978;28:549–551.
5. Lindner M.
Implications of Triviality for the Standard Model.
Z Phys. 1986;C31:295.
6. Wetterich C.
THE MASS OF THE HIGGS PARTICLE.
In: Search for Scalar Particles: Experimental and Theoretical Aspects Trieste, Italy, July 23-24, 1987; 1987. p. 1.
Available from: <http://alice.cern.ch/format/showfull?sysnb=0094536>.
7. Altarelli G, Isidori G.
Lower limit on the Higgs mass in the standard model: An Update.
Phys Lett. 1994;B337:141–144.
8. Schrempp B, Wimmer M.
Top quark and Higgs boson masses: Interplay between infrared and ultraviolet physics.
Prog Part Nucl Phys. 1996;37:1–90.
9. Hambye T, Riessellmann K.
Matching conditions and Higgs mass upper bounds revisited.

- Phys Rev. 1997;D55:7255–7262.
10. Buttazzo D, Degrandi G, Giardino PP, Giudice GF, Sala F, Salvio A, et al. Investigating the near-criticality of the Higgs boson. *JHEP.* 2013;12:089.
 11. Espinosa JR. Implications of the top (and Higgs) mass for vacuum stability. *PoS.* 2016;TOP2015:043.
 12. Bezrukov F, Shaposhnikov M. Why should we care about the top quark Yukawa coupling? *J Exp Theor Phys.* 2015;120:335–343.
 13. Gies H, Gneiting C, Sondenheimer R. Higgs Mass Bounds from Renormalization Flow for a simple Yukawa model. *Phys Rev.* 2014;D89(4):045012.
 14. Gies H, Sondenheimer R. Higgs Mass Bounds from Renormalization Flow for a Higgs-top-bottom model. *Eur Phys J.* 2015;C75(2):68.
 15. Holland K, Kuti J. How light can the Higgs be? *Nucl Phys Proc Suppl.* 2004;129:765–767. [765(2003)].
 16. Holland K. Triviality and the Higgs mass lower bound. *Nucl Phys Proc Suppl.* 2005;140:155–161. [155(2004)].
 17. Branchina V, Faivre H. Effective potential (in)stability and lower bounds on the scalar (Higgs) mass. *Phys Rev.* 2005;D72:065017.
 18. Datta A, Young BL, Zhang X. Implications of a nonstandard light Higgs boson. *Phys Lett.* 1996;B385:225–230.
 19. Barbieri R, Strumia A. What is the limit on the Higgs mass? *Phys Lett.* 1999;B462:144–149.
 20. Grzadkowski B, Wudka J. Bounds on the Higgs-Boson mass in the presence of nonstandard interactions. *Phys Rev Lett.* 2002;88:041802.
 21. Burgess CP, Di Clemente V, Espinosa JR. Effective operators and vacuum instability as heralds of new physics. *JHEP.* 2002;01:041.
 22. Barger V, Han T, Langacker P, McElrath B, Zerwas P. Effects of genuine dimension-six Higgs operators. *Phys Rev.* 2003;D67:115001.
 23. Blum K, D’Agnolo RT, Fan J. Vacuum stability bounds on Higgs coupling deviations in the absence of new bosons. *JHEP.* 2015;03:166.
 24. Wetterich C. Exact evolution equation for the effective potential. *Phys Lett.* 1993;B301:90–94.
 25. Berges J, Tetradis N, Wetterich C. Nonperturbative renormalization flow in quantum field theory and statistical physics. *Phys Rept.* 2002;363:223–386.
 26. Pawłowski JM. Aspects of the functional renormalisation group. *Annals Phys.* 2007;322:2831–2915.
 27. Gies H. Introduction to the functional RG and applications to gauge theories. *Lect Notes Phys.* 2012;852:287–348.
 28. Delamotte B.

- An Introduction to the nonperturbative renormalization group.
Lect Notes Phys. 2012;852:49–132.
29. Braun J.
Fermion Interactions and Universal Behavior in Strongly Interacting Theories.
J Phys. 2012;G39:033001.
 30. Jakovac A, Kaposvari I, Patkos A.
Scalar mass stability bound in a simple Yukawa-theory from renormalization group equations.
Mod Phys Lett. 2016;A32(02):1750011.
 31. Jakovac A, Kaposvari I, Patkos A.
Renormalisation Group determination of scalar mass bounds in a simple Yukawa-model.
Int J Mod Phys. 2016;A31(28n29):1645042.
 32. Gies H, Sondenheimer R, Warschinke M.
Impact of generalized Yukawa interactions on the lower Higgs mass bound. 2017; Available from: <https://inspirehep.net/record/1610026/files/arXiv:1707.04394.pdf>.
 33. Eichhorn A, Gies H, Jaeckel J, Plehn T, Scherer MM, Sondenheimer R.
The Higgs Mass and the Scale of New Physics.
JHEP. 2015;04:022.
 34. Fodor Z, Holland K, Kuti J, Nogradi D, Schroeder C.
New Higgs physics from the lattice.
PoS. 2007;LAT2007:056.
 35. Gerhold P, Jansen K.
The Phase structure of a chirally invariant lattice Higgs-Yukawa model for small and for large values of the Yukawa coupling constant.
JHEP. 2007;09:041.
 36. Gerhold P, Jansen K.
The Phase structure of a chirally invariant lattice Higgs-Yukawa model - numerical simulations.
JHEP. 2007;10:001.
 37. Gerhold P, Jansen K.
Lower Higgs boson mass bounds from a chirally invariant lattice Higgs-Yukawa model with overlap fermions.
JHEP. 2009;07:025.
 38. Hegde P, Jansen K, Lin CJD, Nagy A.
Stabilizing the electroweak vacuum by higher dimensional operators in a Higgs-Yukawa model.
PoS. 2014;LATTICE2013:058.
 39. Chu DYJ, Jansen K, Knippschild B, Lin CJD, Nagy A.
A lattice study of a chirally invariant Higgs-Yukawa model including a higher dimensional ϕ^6 -term.
Phys Lett. 2015;B744:146–152.
 40. Chu DYJ, Jansen K, Knippschild B, Lin CJD, Nagai KI, Nagy A.
Phase structure and Higgs boson mass in a Higgs-Yukawa model with a dimension-6 operator.
PoS. 2014;LATTICE2014:278.
 41. Akerlund O, de Forcrand P.
Higgs-Yukawa model with higher dimension operators via extended mean field theory.
Phys Rev. 2016;D93(3):035015.
 42. Espinosa JR.
Cosmological Implications of Higgs Near-Criticality.
Philosophical Transactions A, this issue. 2017;.
 43. Bednyakov AV, Kniehl BA, Pikelner AF, Veretin OL.
Stability of the Electroweak Vacuum: Gauge Independence and Advanced Precision.
Phys Rev Lett. 2015;115(20):201802.
 44. Alekhin S, Djouadi A, Moch S.
The top quark and Higgs boson masses and the stability of the electroweak vacuum.
Phys Lett. 2012;B716:214–219.
 45. Borchardt J, Gies H, Sondenheimer R.

- Global flow of the Higgs potential in a Yukawa model.
Eur Phys J. 2016;C76(8):472.
46. Litim DF, Pawłowski JM, Vergara L.
Convexity of the effective action from functional flows. 2006; Available from:
https://inspirehep.net/record/710544/files/arXiv:hep-th_0602140.pdf?version=2.
47. Eichhorn A, Scherer MM.
Planck scale, Higgs mass, and scalar dark matter.
Phys Rev. 2014;D90(2):025023.
48. Bezrukov F, Rubio J, Shaposhnikov M.
Living beyond the edge: Higgs inflation and vacuum metastability.
Phys Rev. 2015;D92(8):083512.
49. Moss IG.
Higgs boson cosmology.
Contemp Phys. 2015;56(4):468–476.
50. Espinosa JR, Giudice GF, Morgante E, Riotto A, Senatore L, Strumia A, et al.
The cosmological Higgstory of the vacuum instability.
JHEP. 2015;09:174.
51. Herranen M, Markkanen T, Nurmi S, Rajantie A.
Spacetime curvature and Higgs stability after inflation.
Phys Rev Lett. 2015;115:241301.
52. Markkanen T.
Vacuum Stability in the Early Universe and the Backreaction of Classical Gravity.
Philosophical Transactions A, this issue. 2017; Available from:
<http://inspirehep.net/record/1609614/files/arXiv:1707.03415.pdf>.
53. Akerlund O, de Forcrand P, Steinbauer J.
Effects of higher dimension operators on the Standard Model Higgs sector.
In: Proceedings, 33rd International Symposium on Lattice Field Theory (Lattice 2015); 2015.
Available from: <http://inspirehep.net/record/1404165/files/arXiv:1511.03867.pdf>.
54. Shaposhnikov M, Wetterich C.
Asymptotic safety of gravity and the Higgs boson mass.
Phys Lett. 2010;B683:196–200.
55. Eichhorn A, Held A.
Viability of quantum-gravity induced ultraviolet completions for matter. 2017;.
56. Holdom B, Ren J, Zhang C.
Stable Asymptotically Free Extensions (SAFEs) of the Standard Model.
JHEP. 2015;03:028.
57. Gies H, Zambelli L.
Asymptotically free scaling solutions in non-Abelian Higgs models.
Phys Rev. 2015;D92(2):025016.
58. Gies H, Zambelli L.
Non-Abelian Higgs models: Paving the way for asymptotic freedom.
Phys Rev. 2017;D96(2):025003.
59. Helmboldt AJ, Humbert P, Lindner M, Smirnov J.
Minimal Conformal Extensions of the Higgs Sector. 2016;.
60. Hansen FF, Janowski T, Langaebler K, Mann RB, Sannino F, Steele TG, et al.
Phase structure of complete asymptotically free $SU(N_c)$ theories with quarks and scalar quarks [arXiv:1706.06402]. 2017;.